Estimation of Harmonics in Sparsely Monitored Distribution Networks

Estimation of Harmonics in Sparsely Monitored Distribution Networks

Yuqi Zhao, Jovica V. Milanović
The University of Manchester
Manchester, UK
yuqi.zhao@postgrad.manchester.ac.uk
jovica.milanovic@manchester.ac.uk

***Abstract*— Accurate estimation of harmonics in partially monitored power networks with uncertain, power electronics interfaced low carbon technologies can facilitate efficient planning and operation of future net-zero distribution networks. A recent study demonstrated a methodology for estimating harmonic distortions in partially monitored, typically radial, residential distribution networks. This study extends the general applicability of the harmonic estimation method to higher voltage meshed networks. The Morris screening method based harmonic variation sensitivity analysis, and the sensitivity method based on electrical distance were proposed in this study and were combined together to determine the optimal/minimum number and location of PQ monitors. Appropriate scaling factors were recommended as well. This solves the problem of sub-optimal selection of monitoring locations when harmonic distortion is not highly correlated with the voltage drop at buses in the meshed network. Different types of harmonic injections from nonlinear loads are fitted using Kernel non-parametric distribution and are estimated separately according to different load types. The approach is validated, and its accuracy and reliability were demonstrated on a highly interconnected (meshed) section of the power system.**

***Keywords*— Harmonic estimation, meshed network, sparsely monitored system, uncertainties, power electronics, power quality, probabilistic analysis**

I. INTRODUCTION

As the goal to reach Net Zero carbon emissions by 2050 rapidly approaches, the UK government has announced a package of 18 deals worth £9.7 billion to support green growth on top of the £5.8 billion already committed for sustainable projects [1]. To achieve this, a large amount of non-conventional, renewable generations (e.g., 40GW of offshore wind by 2030, with more onshore, solar, and other renewables) and storage technologies will be connected to the power system through power electronic (PE) devices. At the same time, the reliance on PE-connected technologies, such as voltage source converter-based high voltage direct current (VSC-HVDC) lines, line commutated converter-based high voltage direct current (LCC-HVDC) transmission lines, and flexible alternating current transmission systems (FACTS), will increase, typically in meshed networks, to enhance the efficiency and security of the power supply. In view of the customer side, the increasing utilization of PE based/connected loads (e.g., heat pumps and lighting) and electric vehicles (EVs) charging have been foreseen [1, 2].

The proliferation of these PE switching devices amplifies the non-sinusoidal disturbance of the power system, challenging the monitoring of power quality (PQ) issues, especially the harmonic distortion issues which result in uncontrolled component overheating, additional power losses, and significant financial losses [2, 3]. Moreover, since the renewable generations are largely stochastic and intermittent in nature, and the EVs tend to be affected by spatial and temporal uncertainties, the harmonic phenomena will be more pronounced in future power gird.

In order to effectively anticipate and mitigate harmonic problems, the harmonic state estimation (HSE) method [4] has been widely explored in transmission networks [5-7] and in radial distribution networks [8-10]. A recent study [10] demonstrated a methodology for estimating harmonic distortions in partially monitored, typically radial, residential distribution networks. Even though this method has been shown to be very effective and reliable, it remains challenging to implement it directly to meshed networks in two aspects:

i. The correlation between the harmonic voltage levels and the voltage-drop levels defined in [10] is not obvious at buses in the meshed network due to the higher complexity of the power flows.

ii. The non-linear (NL) loads are commonly categorized into different types in the meshed network, e.g., commercial type, and domestic type. It is more realistic to estimate harmonic injections according to different load types.

Building on [10], this paper proposes an alternative method to solve the problem of sub-optimal selection of monitoring locations when harmonic distortion is not highly correlated with the voltage drop at buses in the meshed network. To obtain a more accurate estimation of harmonic current injections, the harmonic distortions from nonlinear loads are fitted and estimated separately according to different load types.

The approach was demonstrated using a combination of MATLAB (estimation) and DigSILENT/PowerFactory (network modeling and probabilistic Monte Carlo (MC) simulations to account for various operating scenarios and associated uncertainties) simulation environment [11].

II. METHODOLOGY

A. Overview

To estimate harmonic distortions across the whole meshed network, harmonic measurements at a small subset of monitored buses are used and the results are extrapolated to unmonitored buses. Fig.1 summarizes the information required before and during the harmonic estimation. At stage one, the simulations are carried out once until the optimal locations of PQ monitors are obtained. The information required for this process is (in the yellow box): weekly voltage profile (1st harmonic only) at all buses, system configuration, and relevant system parameters (this is not necessarily required).

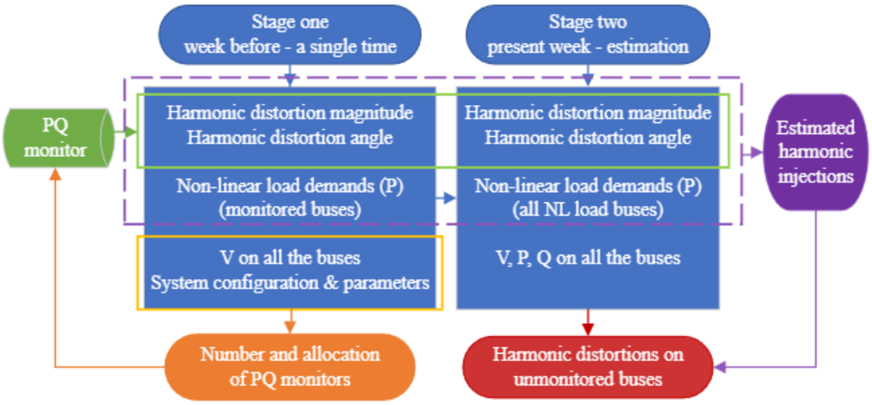

Fig. 1. Required information for proposed harmonic estimation methodology.

At stage two, the harmonic injections at all the NL load buses are first estimated. The information required for this process are (in the purple box): the harmonic measurements from installed PQ monitors (in the green box), together with the NL load demands. The active power of NL loads can be obtained by the conventional meters or assumed to be predicted in advance as in [12]. Then, with the real-time information on V, P and Q profiles at all network buses, the harmonic distortions at all unmonitored buses can be calculated based on the adopted algorithm as in [10].

B. PQ Monitor Location

Accurate voltage harmonic estimation in a realistic network requires the identification of the optimal number and location of PQ monitors. Since these monitors are assumed to be installed at/selected from buses connected to NL loads (the assumption is kept throughout this study), the key issue of this monitor location approach involves placing a PQ monitor at a representative bus in each group of buses that have:

a) *Short electrical distance from monitored buses* and *high sensitivity of voltage variations* to voltage drops at the monitored buses.

b) *High sensitivity of harmonic variations* at unmonitored buses with respect to the harmonic distortions injected at the monitored load buses.

C. Electrical Distance Sensitivity

Electrical distance plays a significant role in power system analysis, aiding in the identification of internal and external connections between buses [9, 13]. The extent of interaction between buses is largely dependent on the magnitude of electrical distance. This study utilizes a sensitivity-based method (SM) [13] to simplify computational complexity while calculating electrical distance. The degree of voltage coupling between node *i* and node *j* is measured through the attenuation of voltage variations between them (ΔV_i, ΔV_j), represented by equation (1).

$$\alpha_{i,j} = \frac{\Delta V_i}{\Delta V_j} \tag{1}$$

where α_{ij} represents voltage variations at node *i* (selected from all buses) with respect to the perturbation on node *j* (selected from NL load buses). A smaller α_{ij} represents weaker electrical connection between the two nodes.

In this study, to accommodate different system operating conditions and system uncertainties, α_{ij} is calculated as the average values of voltage variations during the entire sampling time span (*T*), as in equation (2).

$$\alpha_{i,j} = \frac{1}{T-1}\sum_{t=1}^{T-1}\left|\frac{V_i^t - V_i^{t+1}}{V_j^t - V_j^{t+1}}\right| \tag{2}$$

In theory, the electrical distance between the bus *i* and bus *j* when *i=j*, *α =1*, should be the shortest. Therefore, the logarithm is utilised to standardise α and thus the equation can be expressed as:

$$d_{i,j} = \left|log\ (\alpha_{i,j})\right| \tag{3}$$

where $d_{i,j}$ represent the electrical distance between node *i* and node *j*. The more $d_{i,j}$ is approaching 0, the shorter the electrical distance between node *i* and node *j*.

Following this, a *sensitivity-based electrical distance matrix* (M_v) can be calculated, which reflects the connection level between all the buses in the network (including buses with NL load and the rest of the buses).

D. Harmonic Sensitivity Analysis

Morris screening method, which identifies and ranks the input parameters according to their influence on the output parameters [14], is applied to perform harmonic sensitivity analysis (#SA). It introduces a *Δ* change in each variable, one at a time. The definition of the elementary effect (EE) of a *Δ* change in the i^{th} factor at a certain position *x* is defined by (4).

$$EE_p^i(x) = \frac{y(x_1,\dots x_{i-1},x_i+\Delta,x_{i+1},\dots,x_k)-y(x)}{\Delta} \tag{4}$$

where *x* is a point chosen from the input region so that the disturbed point, $x + \Delta$, remains in the input region. Since *r* is the total number of permutations, the step size Δ is calculated as a multiple of *1/(r-1)*. For each Morris simulation, a trajectory is constructed where only one variable is varied by Δ in each step, while the values of other variables remain constant. After each step, another variable is randomly selected, and the process is repeated until each variable has undergone *r* steps. To obtain the trajectory, a starting point is selected for each uncertainty by randomly choosing a base value between *Δ* and *1-Δ*. This enables the creation of an input trajectory in the uncertain parameter space [14].

For example, in this study, there are 9 input parameters, which represent the variation of harmonic injections from 9 NL loads. It is assumed that the input range of individual harmonic currents is 0%-3%, the level *r=4*, and the step size Δ is calculated by multiplying the value of the range of inputs by *1/(r-1)*, which is Δ= 3×1/(4-1)= 1%. Therefore, 9 × 4 + 1 = 37 simulations are required. The trajectory of harmonic current injection changes at each load bus is generated randomly using MATLAB.

At different simulation steps, the harmonic magnitude injections from non-linear loads are set as different fixed values based on the MATLAB trajectory, the same for all the harmonic orders. Meanwhile, in order to eliminate the influence of all the other harmonic sources in the entire system, including both distribution loads and generations, the corresponding harmonic injections (both magnitude and phase angle) are set as 0%.

One index to evaluate the elementary effects of each input variable is the mean value (μ), as defined in (5). μ expresses the sensitivity strength between the p^{th} input variable and the output. A high value of μ demonstrates a high contribution of the input to the output, which means the uncertain parameter is more influential [14].

$$\mu = \frac{1}{r}\sum_{i=1}^{r}\left|EE_p^i\right| \quad (5)$$

In this study, to accommodate different system operating conditions and system uncertainties, the final mean values are calculated as the average values of the entire sampling period.

Following this, a *sensitivity-based mean value matrix (M_h)* can be calculated, which reflects the influence of harmonic distortions at NL load buses and all other buses in the system.

E. Optimal PQ Monitor Locations and Bus Clustering

The basic idea of this monitor location method relies on placing a PQ monitor in each group of buses with high sensitivity of both harmonic variations and voltage disturbances among them. In order to establish the appropriate PQ monitor placement and to cluster different unmonitored buses into the monitored group, the following steps are as taken:

i. In order to account for the combined effect of the index M_v and M_h, they are combined proportionally as in the summation equation (6) below.

$$k_h M_h + (1-k_h)M_v = M_{cb} \quad (6)$$

where the scaling factor k_h represents the participation of the SA-based harmonic index M_h into the combined index M_{cb}. With the increase of k_h, the harmonic fluctuations at NL load buses become more influential on finding optimal PQ monitor locations, the bus grouping results, and the final estimation accuracy, and vice versa.

ii. A threshold (λ_{cb}) was applied to classify the M_{cb} into 0 and 1. M_{cb}=1 (true value) means that the corresponding bus and the NL load bus are highly correlated. The value of λ_{cb} is decreased from the max value to the min value in 20 steps so that different matrices (C_{cb}) of classified sensitivity ranking can be obtained.

iii. Following each step decrease of λ_{cb}, an optimization process is run to identify the smallest number/best location of PQ monitors. This solution ensures that all the buses (rows in matrix C_{cb}) are covered by at least one true value when considering only the selected monitored load buses (columns in the matrix C_{cb}). The position represented by these selected columns is the optimal solution for placing the PQ monitors. The detailed optimization algorithm can be found in [10].

iv. Then the buses highly correlated to the monitored buses (true values in the selected columns) are clustered into the same group. In other words, each group consists of one monitored bus and its correlated buses.

v. In order to avoid duplicate assignments of the same bus, if an unmonitored bus is highly correlated to multiple monitored buses, it will be assigned to the cluster where the bus with the higher value of M_{cb} is located. If, however, a monitored bus is also correlated to any other monitored bus it will be removed from the other bus groups.

It is important to note that the procedure to locate PQ monitors is performed just once prior to the estimation and can be continuously utilised until the general system topology changes, which does not commonly happen in the medium/higher-voltage distribution/sub-transmission meshed networks. The PQ monitor locations are not reliant on specific bus location, but rather on the relative electrical distance between buses.

F. Harmonic Estimation

In order to obtain a more accurate estimation of harmonic current injections from different types of NL loads, this study fits the harmonic measurements separately according to different load types. The estimated values are combined according to their share in the total demand at the bus. Kernel non-parametric (KNP) distribution is utilised for fitting and estimation. The parameters of KNP distributions are determined by the power demand (to estimate harmonic magnitude) and the harmonic currents (to estimate harmonic phase angle) measured by PQ monitors. The harmonic estimation methodology is detailed in [10]. Given that both the magnitude and the phase angle of all individual harmonic injections have been estimated, the method can be generally applied for the harmonic cancellation, amplification, and attenuation studies.

Estimation of harmonic voltage distortions at unmonitored buses is then performed following the methodology proposed in [10,], with the equations below.

$$k_{ij} \simeq (V_j - V_i)/I_{ji} \quad (7)$$

$$I_{ij} \simeq \sqrt{\sum_{k=j}^{n}(P_k^2 + Q_k^2)}\,/V_j \quad (8)$$

$$k_{i,j}^h = k_{i,j}(R + jhX) \quad (9)$$

$$\sqrt{R^2 + X^2} = 1 \quad (10)$$

$$V_j^h = V_i^h + k_{i,j}^h \sum_{k=j}^{Nr} I_k^h \quad (11)$$

where V_i and V_j represent the voltage at the adjacent buses i and j, respectively. Current I_{ij} represents the equivalent total current injected from bus j to i, which is calculated by considering the cumulative active power P and reactive power Q flowing from bus j to the most electrically distant bus n. The parameter k_{ij} stands for the equivalent impedance between node i and node j and therefore has the impedance unit (Ω). In order to consider harmonic frequencies, the coefficient $k_{i,j}^h$ is updated and transformed into complex numbers by multiplying an equivalent harmonic model characterized by by the harmonic order h, resistance R, and reactance X. At the end, the harmonic voltages at a non-monitored bus j, represented as V_j^h, can be calculate using equation (11) where V_i^h represents the harmonic voltage distortion at the monitored bus i, $k_{i,j}^h$ can be derived from equation (9) and

(10), and I_k^h equals to the estimated harmonic current injections from non-linear load buses.

In this way, the harmonic voltages at the other non-monitored bus, for example, bus *j+1*, can be subsequently calculated by assuming all the relevant parameters at bus *j* are available. Thus, by repeatedly applying equation (5) to the buses located electrically further away from the monitored bus, all the harmonic voltages can be estimated sequentially for all the non-monitored system buses.

III. Test Network

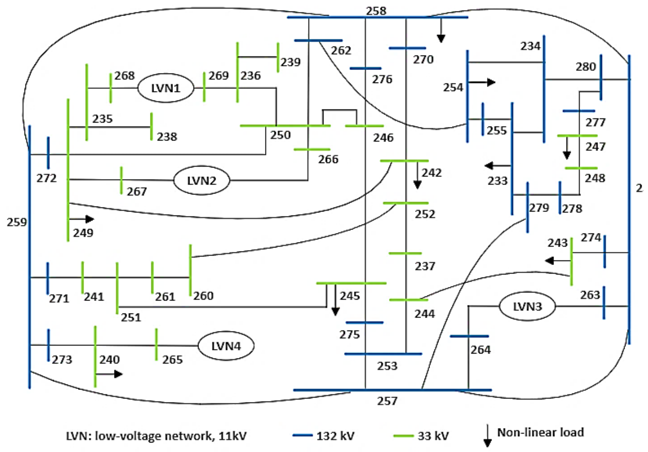

Fig. 2. Simplified 48-bus meshed section of the modified 295-bus GDN.

The GDN network was widely used in various types of studies in the past [15-17]. The network parameters were modelled based on realistic UK distribution networks. The annual hourly loading curves were extracted from the year 2010 survey of different types of loads. A detailed description of modelling of network parameters and distribution generator (DG) outputs can be found in [17].

Different types of non-linear loads and DGs were modelled probabilistically as harmonic current sources. As required in the IEC Standard 61000-3-6 [18] and the Engineering Recommendation G5/4 [19], a total of 50 harmonics were modelled for planning and controlling purposes. The range of individual harmonic-order injections was selected based on the long–term measurements and on the harmonic spectrum of PE interfaced components reported in [2, 6, 7, 18, 19]. For the wind, solar, and storage, the harmonic magnitude injections were randomly sampled from uniformly distributed ranges as utilised in [6,7]. For the NL loads, the harmonic magnitude injections were randomly sampled from uniformly distributed ranges from 0 to the values specified in standard G5/4 [19]. The NL loads are composed of 80% domestic load (D type) and 20% commercial load (C type). All the harmonic angle injections were randomly sampled using uniform distribution within a range of (0°, 180°). The simulations were performed using Monte Carlo approach that considers the uncertainties resulting from the non-linear portions of loads and the changing switching frequency of converters. In accordance with standard EN50160 [20], the assessments of harmonics were performed considering weekly evaluation, with a 10-mins time-step.

It should be noted that even if this study concentrates on discussing the harmonic estimation of only the meshed section of the GDN, the simulations were performed based on the operation of the entire GDN, i.e., all NL loads and distributed generations connected at different voltage levels were considered during simulations, thus influencing the harmonic propagations throughout the network.

IV. Case Study

A. Base Case

The proposed methodology is initially (Case 1.1) implemented in the meshed sections of the network surrounded by 132 kV voltage level. The fitted cumulative distribution function (CDFs) of total harmonic distortions (THD) absolute estimation errors (= estimated values – actual values) at all test network buses is illustrated in Fig. 3. The results indicate that the majority of the mean values of fitted absolute errors are centred around 0%, and during 95% of the observation period, the total absolute errors are less than 0.05%. Therefore, these findings provide compelling evidence that the proposed model is sufficiently accurate in estimating THD at unmonitored buses.

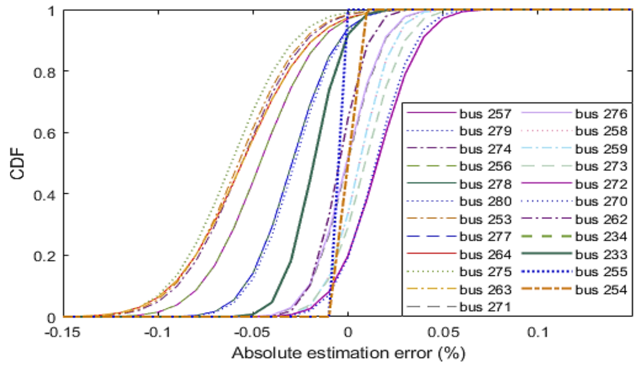

Fig. 3. Fitted CDFs of absolute estimation errors of THD for Case 1.1.

Boxplots comparing estimated and real THD values at various unmonitored buses for Case 1.1 are presented in Fig. 4. A notable observation is that the medians, width, and boundaries of both actual and estimated THD values are largely overlapping for the majority of the buses. This strongly suggests that the estimated THD value distributions closely align with their actual values, thus providing further validation of the broad applicability of the proposed methodologies in harmonic estimation for meshed networks.

B. Effect of the Estimated Harmonic Injections

In order to investigate the effect of modelling different types of harmonic injections, two cases are considered. In Case 2.1, the harmonic measurements obtained from PQ monitors are fitted in segments using KNP distribution. Based on the fitted distribution, the harmonic injections from unmonitored NL loads are estimated by segments, regardless of load type. In case 2.2, the PQ measurements are separately fitted for the C-type loads and D type of loads. Then the harmonic injections from both types of loads are estimated based on different distributions and are combined together according to their corresponding proportions at the NL loads. Table I summarises the average mean values of the absolute estimation errors and the average 95th absolute estimation errors among all the buses.

It can be seen that when estimating harmonic injections without considering different harmonic distributions for different load types, the mean values of error distribution will increase and the 95th estimation errors will be amplified. Therefore, the appropriate harmonic distributions should be fitted, and the harmonic injections should be estimated by considering different NL load types.

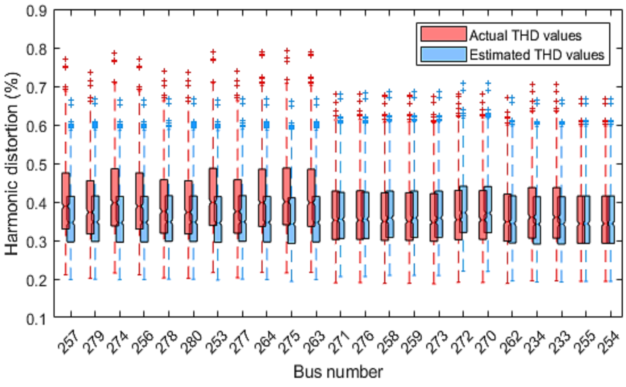

Fig. 4. Boxplots of THD values for Case 1.1.

TABLE I. AVERAGE MEAN VALUE AND 95TH ABSOLUTE ESTIMATION ERROR FOR CASE 2.1-CASE 2.3.

Case no.	Average 95th absolute estimation error	Average mean value
Case 2.1	0.105%	0.074%
Case 2.2	0.060%	0.029%
Case 2.3	0.058%	0.028%

As one of the factors that influence the estimation accuracy of the final harmonic distortions at unmonitored buses, the process of estimating harmonic injections at NL loads has to be evaluated. To realise this, in Case 2.3, the harmonic injections from unmonitored NL load buses obtained by sampling corresponding probability distributions are replaced with the actual values. The corresponding results can be found in Table I. Compared with Case 2.2, Case 2.3 results in very similar average mean values and 95th estimation errors. Therefore, the estimated harmonic injections are sufficiently accurate so that the final accuracy will not be affected by it when estimating the THD at unmonitored buses.

C. *Effect of the Scaling Factor k_h*

Since the proposed methodology introduces a scaling factor k_h to represent the participation of the SA-based harmonic index M_h into the combined raking index, it is necessary to investigate its influence on the estimation accuracy. Therefore, the harmonic distortions at unmonitored buses were estimated while increasing gradually the scaling factor k_h from 0 to 1. Fig. 5 plots the average 95th absolute estimation errors at all unmonitored buses and the corresponding required number of PQ monitors with respect to scaling factor k_h.

It can be seen that the average 95th absolute estimation error initially slightly increases from 0.05% to 0.06% when k_h is increasing from 0 to 0.2, then the error keeps decreasing to 0.04% and then sharply increases when k_h increases to 0.77. Once the k_h reaches the knee point of 0.78, the estimation error increases to 0.51% and pretty much stays at that level (approx. 0.53%) for further increase in k_h. The number of the required PQ monitors tends to be larger with a higher k_h. In this case study, two PQ monitors are required to be installed in this system so that the harmonic distortions at all the unmonitored buses could be estimated more accurately.

Therefore, in practical application, it is recommended to set the scaling factor R_h to lower values (approximately 0.2 to 0.77) to achieve the best estimation accuracy with the lowest number of PQ monitors. The sensitivity-based harmonic distortion matrix (M_h) should not be used independently since it will result in relatively large errors in THD estimation. However, if the configuration and the parameters of the system are not accessible in advance, i.e., M_h is unavailable, the sensitivity-based electrical distance matrix (M_v) can be used independently as it will result in higher estimation accuracy than if M_h was used independently.

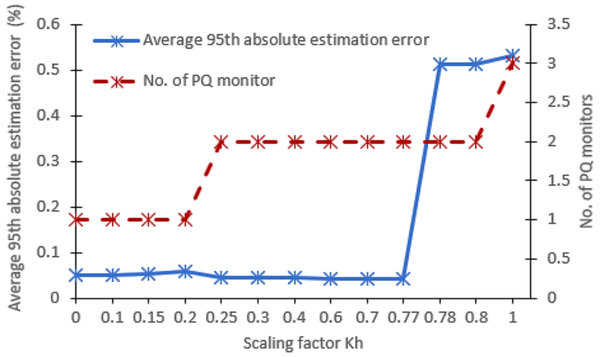

Fig. 5. Average 95th absolute estimation errors and required number of PQ monitors with respect to the scaling factor k_h.

D. *Validation of the Model*

In order to validate the general applicability of the proposed methodology, harmonic measurements have been obtained by simulating the entire 48-buses meshed GDN test network. The proposed methodology is then applied to estimate the harmonic distortions at all unmonitored buses in the entire meshed section of the test GDN. The boxplots of absolute estimation errors of THD are shown in Fig.6. The boxplots of THD values are compared in Fig. 7.

In this case, four PQ monitors are required to be installed at Bus 242, Bus 243, Bus 247, and Bus 258, i.e., at approximately 8% (4/48) of the buses in the network. More PQ monitors are required in this case as there are more NL load buses, as well as more unmonitored buses in the 48-bus meshed GDN. Based on the harmonic measurements obtained from these monitors, the harmonic injections at NL load buses and the harmonic distortions at all the unmonitored buses can be estimated sequentially. The average mean value of the absolute estimation errors is 0.14% and the average 95th absolute estimation error is 0.24%. According to standard IEC TR 61000-3-6 [18], both of the estimation errors are relatively insignificant compared with the 3% THD limit at the 132 kV system and the 6.5% THD limit at the 33 kV system.

It can be seen from Fig. 7 that the boxplots of estimated and actual THD values are approximately overlapped, which proves that the estimated THD values are following the same trend as their actual harmonic variations. Meanwhile, it can be seen from Fig. 6 that for the majority (36/48=75%) of the buses, the error distributions and mean values are concentrated at approximately 0%, which indicates extremely high estimation accuracy. At the same time, for some (9/48=19%) buses, the mean values of absolute estimation errors are concentrated at approximately -0.4% and are distributed narrowly, i.e., the error range from 25th to 75th is within 0.5%. Only three buses (Bus 265, Bus 240, and Bus 249) had the harmonic distortions relatively larger than the others. According to Fig.2, this is because these buses are connected to the branch where a low-voltage network is connected downstream and continuously brings up the harmonic distortion levels at the upstream buses. The closer the bus is to the low voltage distribution network, the higher is the influence of low voltage connected PE and other NL devices and consequently higher harmonic propagation fluctuations and potentially onset of harmonic resonance. These factors will increase the risk of over/under estimation. However, when compared with the 6.5% of THD limit in a lower voltage system, the worst 95th absolute estimation error is only about 5% (0.35/6.5) of the THD limit which is completely acceptable.

Therefore, the proposed harmonic estimation methodology performs well and can be used to estimate the harmonic distortions at unmonitored buses in a non-radial network with multiple voltage levels with a good accuracy. To be more specific, an accurate estimation can be obtained at 94% of the unmonitored buses by installing PQ monitors at approximately 8% of network buses.

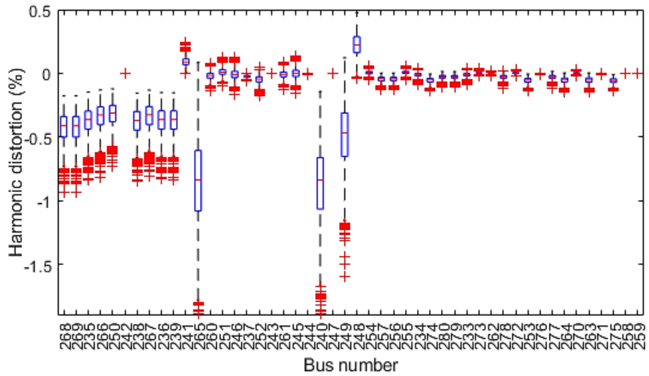

Fig. 6. Boxplots of absolute estimation errors for meshed GDN.

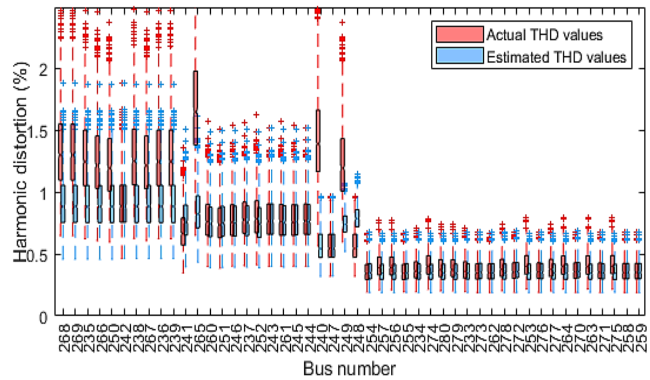

Fig. 7. Boxplots of THD values for meshed GDN.

V. Conclusion

This study extends the general applicability of the harmonic estimation method proposed in [10] from typical radial residential distribution networks to higher voltage meshed distribution networks. The approach facilitates the assessment of standard compliance, reduces the extent of monitor installations in the network, accelerates the assessment of harmonic performance and mitigation in uncertain networks, and contributes to the forecast of potential harmonic issues in future power networks.

Acknowledgment

This work was partly supported by Grant RTI2018-097424-B-I00 funded by MCIN/AEI/10.13039/501100011033 and by “ERDF A way of making Europe". The authors acknowledge enlightening discussions and helpful suggestions by our project partners Assoc. Prof Araceli Hernández Bayo and Dr Pablo Rodríguez-Pajarón.

References

[1] Department for Business, Energy & Industrial Strategy, U.K., *Net Zero Strategy: Build Back Greener*. Oct 2021. [Online]. Available: https://assets.publishing.service.gov.uk/government/uploads/system/uploads/attachment_data/file/1033990/net-zero-strategy-beis.pdf

[2] Y. Zhao and J. V. Milanović, "Equivalent Modelling of Wind Farms for Probabilistic Harmonic Propagation Studies," *IEEE Transactions on Power Delivery*, vol. 37, no. 1, pp. 603-611, Feb. 2022.

[3] G. J. Wakileh, *Power Systems Harmonics: Fundamentals, Analysis and Filter Design*. New York, NY, USA; Berlin, Germany: Springer, 2001.

[4] S. K. Jain and S. Singh, "Harmonics estimation in emerging power system: Key issues and challenges," *Electric power systems research*, vol. 81, no. 9, pp. 1754-1766, 2011.

[5] A. S. Meliopoulos, F. Zhang, and S. Zelingher, "Power system harmonic state estimation," *IEEE Transactions on Power Delivery*, vol. 9, no. 3, pp. 1701-1709, 1994.

[6] Y. Zhao and J. V. Milanović, "Probabilistic Harmonic Estimation in Uncertain Transmission Networks Using Sequential ANNs," *2022 20th International Conference on Harmonics & Quality of Power (ICHQP)*, Naples, Italy, pp. 1-6, 2022.

[7] Y. Zhao, J. V. Milanović, P. Rodríguez-Pajarón and A. Hernández, "Accuracy of Probabilistic Harmonic Estimation in Sparsely Monitored Transmission Networks," *2022 17th International Conference on Probabilistic Methods Applied to Power Systems (PMAPS)*, Manchester, United Kingdom, pp. 1-6, 2022.

[8] X. Xiao, Z. Li, Y. Wang, and Y. Zhou, "A Practical Approach to Estimate Harmonic Distortions in Residential Distribution System," *IEEE Transactions on Power Delivery*, vol. 36, Jun. 2021.

[9] S. Abdelrahman and J. V. Milanović, "Practical Approaches to Assessment of Harmonics Along Radial Distribution Feeders," in *IEEE Transactions on Power Delivery*, vol. 34, no. 3, pp. 1184-1192, June 2019.

[10] P. Rodríguez-Pajarón, A. Hernández and J. V. Milanović, "Estimation of Harmonics in Partly Monitored Residential Distribution Networks With Unknown Parameters and Topology," in *IEEE Transactions on Smart Grid*, vol. 13, no. 4, pp. 3014-3027, July 2022.

[11] DIgSILENT PowerFactory User Manual. DIgSILENT GmbH, 2021.

[12] J. Ponoćko and J. V. Milanović, "Forecasting Demand Flexibility of Aggregated Residential Load Using Smart Meter Data," in *IEEE Transactions on Power Systems*, vol. 33, no. 5, pp. 5446-5455, Sept. 2018, doi: 10.1109/TPWRS.2018.2799903.

[13] X. Mao, W. Zhu, L. Wu, and B. Zhou, "Comparative study on methods for computing electrical distance," *International Journal of Electrical Power & Energy Systems*, vol. 130, p. 106923, 2021.

[14] K. N. Hasan, R. Preece and J. V. Milanović, "Priority Ranking of Critical Uncertainties Affecting Small-Disturbance Stability Using Sensitivity Analysis Techniques," in *IEEE Transactions on Power Systems*, vol. 32, no. 4, pp. 2629-2639, July 2017.

[15] S. Bahadoorsingh, J. V. Milanovic, Y. Zhang, C. P. Gupta and J. Dragovic, "Minimization of Voltage Sag Costs by Optimal Reconfiguration of Distribution Network Using Genetic Algorithms," in *IEEE Transactions on Power Delivery*, vol. 22, no. 4, pp. 2271-2278, Oct. 2007.

[16] H. Liao, S. Abdelrahman and J. V. Milanović, "Zonal Mitigation of Power Quality Using FACTS Devices for Provision of Differentiated Quality of Electricity Supply in Networks With Renewable Generation," in *IEEE Transactions on Power Delivery*, vol. 32, no. 4, pp. 1975-1985, Aug. 2017.

[17] S. Abdelrahman, H. Liao, J. Yu and J. V. Milanovic, "Probabilistic assessment of the impact of distributed generation and non-linear load on harmonic propagation in power networks," *2014 Power Systems Computation Conference*, Wroclaw, Poland, pp. 1-7, 2014.

[18] IEC Standard 61000-3-6, “Electromagnetic compatibility (EMC)-Limits - Assessment of emission limits for the connection of distorting installations to MV, HV and EHV power systems,” 2008.

[19] Engineering Recommendation G5/4, “Planning levels for harmonic voltage distortion and the connection of non-linear equipment to transmission systems and distribution network in the UK,” 2005.

[20] EN50160, "Voltage Characteristics of Electricity Supplied by Public Distribution Networks," 2010.